TAILORING OPTICAL CHARACTERISTICS OF DISPERSION-SHIFTED LIGHTGUIDES FOR APPLICATIONS NEAR 1.55 μm

William A. Reed, Leonard G. Cohen, and Hen-Tai Shang

William A. Reed, ***Leonard G. Cohen,*** *and* ***Hen-Tai Shang*** *are with AT&T Bell Laboratories.* ***Mr. Reed*** *is a distinguished member of the technical staff in the Glass Research and Development Department at Murray Hill. He joined AT&T in 1961 and currently works on the design and characterization of optical waveguides. He received the B.S. from Oberlin College and the Ph.D. from Northwestern University, both in physics.* ***Mr. Cohen*** *is supervisor of the Lightguide Materials, Diagnostics, and Applications Group in the Glass Research and Development Department at Murray Hill, New Jersey. He joined AT&T in 1968. He received the B.E.E. degree from City College, City University of New York, and Sc.M. and Ph.D. degrees from Brown University.* ***Mr. Shang*** *is a member of the technical staff at Norcross, Georgia, in the* (continued on page 122)

Next-generation single-mode lightguides may be used in the 1.55-μm wavelength region where losses are a minimum for silica-based fibers. This paper discusses the basic fiber requirements of these new systems and provides design parameters for three types of dispersion-shifted fibers with various graded-index core profiles. The generic structural differences are that one type has a continuous cladding; the second has a depressed-cladding index relative to an outer substrate layer; and the third type has up to four cladding layers with different index values. The latter type includes a new lightguide structure that has a narrow depressed-index trench within its cladding. Results show how to choose lightguide parameters in order to tailor dispersion and mode-confinement properties.

Introduction

Single-mode fibers serve as transmission media for lightguide systems that send data at high rates over long distances. First-generation single-mode fibers are now routinely produced with low losses and zero dispersion near 1.3-μm wavelength (Figure 1) for undersea and terrestrial lightwave system applications. However, future systems may include 1.55 μm wavelength applications because the intrinsic scattering losses in fused silica decrease rapidly with increasing wavelength before reaching a minimum value for $1.5 < \lambda < 1.6$ μm (Figure 1a).

Current research programs use two strategies for optimizing the transmission properties of single-mode fibers that could be used for 1.55-μm wavelength applications. One strategy is to tailor refractive-index profile shapes such that the fibers have low dispersion at wavelengths near 1.55 μm. These fibers can transmit data at high bit rates using injection lasers that emit several longitudinal modes within a narrow spectrum of wavelengths. An alternate design strategy is to remove the low-dispersion constraint and minimize the fiber losses near $\lambda = 1.55$ μm. High bandwidth systems applications near $\lambda = 1.55$ μm

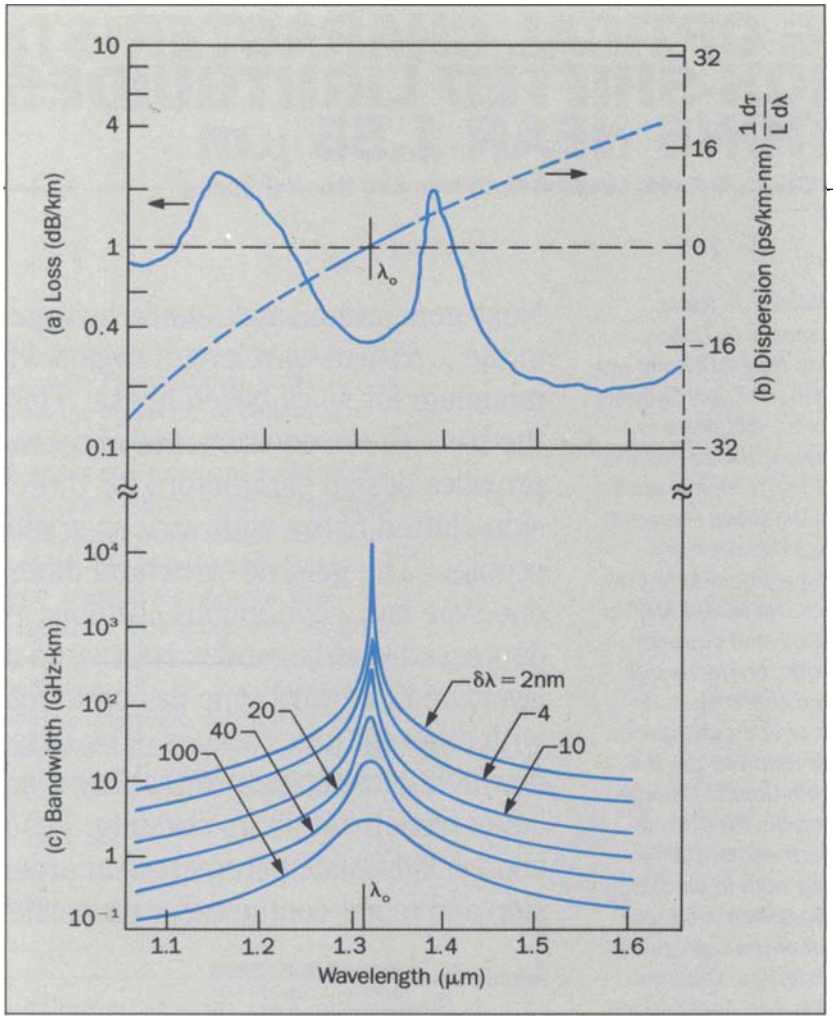

Figure 1. Typical (a) loss, (b) dispersion, and (c) bandwidth of a single-mode fiber with λ_o = 1.3 μm. In (c) δλ is the linewidth of the light source.

would then require the use of single-frequency lasers.

The purpose of this paper is to provide a comprehensive study of the design of dispersion-shifted fibers for use in systems operating in the 1.55-μm wavelength region. The next section illustrates system limitations for high-capacity applications and shows that dispersion-shifted fibers can play an important role for very-long-distance applications. Subsequent sections summarize our computer-aided-modeling studies that were used to enhance the understanding of propagation characteristics and aid the choice of lightguide parameters. It also suggests lightguide modifications that could improve future performance.

Transmission Limitations of High-Capacity Systems

In order to better understand the need for dispersion control in optical fibers it is helpful to review the transmission limitations of high-capacity systems. As the data rate increases in a pulse-code modulation communication system, dispersion effects cause errors which cannot be compensated by increasing the signal power.[1,2] Temporal broadening in single-mode fibers, σ, occurs because chromatic dispersion effects make different wavelengths (frequencies) of an optical pulse propagate with different velocities such that

$$\sigma = DL\delta\lambda \tag{1}$$

where D is the fiber dispersion, L is the fiber length, and δλ is the linewidth of the pulse. The ultimate dispersion limitation of a system can be characterized by convolving

the dispersion spectrum [D (λ) in ps/km-nm] of the fiber (Figure 1b) with the spectrum of an input pulse with linewidth $\delta\lambda$. Minimum pulse broadening (σ_{min}) occurs for a source centered about the zero dispersion wavelength, λ_o, and is proportional to the slope of the dispersion spectrum multiplied by the square of the source linewidth,[3] i.e.,

$$\sigma_{min} \approx \frac{1}{8}\frac{dD}{d\lambda} L\,\delta\lambda^2 \qquad (2)$$

We assume that the dispersion power penalty is small provided that pulse broadening (σ) is smaller than half a bit period ($B \approx 1.82B_w < L/2\sigma$). The bit-rate capacity (B) and bandwidth (B_w) spectra of fibers are inversely related to dispersion as shown in Figure 1c. The peak value of B_w and B increases as $\delta\lambda^2$, and B_w is on the order of 10^4 GHz-km at λ_o. The bandwidth decreases rapidly with wavelength and is only about 30 GHz-km near $\lambda = 1.55$ μm for conventional fiber[4] ($\lambda_o \approx 1.3$ μm) and $\delta\lambda = 2$ nm. Typical single-transverse-mode injection laser sources emit power in several longitudinal modes that are separated by about $\Delta\lambda = 1$ nm in wavelength.

The maximum capacity of a lightwave system is then limited by a combination of dispersion effects, including intersymbol interference due to pulse broadening[1-4] and fluctuations in the received signal due to laser-mode-partitioning.[5] The latter effect occurs because the instantaneous power in any mode can fluctuate randomly with time even if the sum of the power in all laser modes is constant. Such random mode fluctuations add noise to the received signal as they become dispersed in time after propagating along a fiber.

The quality of the laser source may be parameterized by the rms width, $2\delta\lambda$, of the laser spectrum and the fraction, K, of the fluctuation power not in its dominant mode. System performance limits can then be represented by a bit-rate-distance product (BL) that depends upon the $\delta\lambda$ and K parameters of the laser and the chromatic dispersion properties, D and $dD/d\lambda$, of the fiber.[1] Even single-frequency lasers, which emit only one longitudinal mode, can have rapid wavelength variations of that mode with time because of carrier-density changes due to high-frequency injection current pulses. Such chirped behavior causes an effective linewidth broadening ($\delta\lambda \approx 0.1$ nm) of a single-longitudinal mode.[6] Equation (3) represents pulse broadening effects on BL. If several additional longitudinal modes exist, then mode-partition-noise can impose even more stringent performance limitations on BL. For example, if $K > 0.1$ and λ is displaced from the wavelength of minimum dispersion, then pulse broadening effects are represented by equation (4). The BL limitation for the system is the lesser of equation (3) or (4):

$$BL \leq \frac{341}{\delta\lambda D}\frac{\text{Gb-km}}{\text{s}} \qquad (3)$$

$$BL \leq \frac{130}{\delta\lambda D K^{1/2}}\frac{\text{Gb-km}}{\text{s}} \qquad (4)$$

Much higher BL products are possible in dispersion-shifted fibers if λ is close to the system operating wavelength. Then $D \approx 0$ and $\sigma \approx (dD/d\lambda)L\delta\lambda^2$ (instead of $DL\delta\lambda$) which leads to dispersion constraints given by either equation (5) or (6), whichever is smaller:

$$BL \leq \frac{11207}{\delta\lambda^2\frac{dD}{d\lambda}}\frac{\text{Gb-km}}{\text{s}} \qquad (5)$$

$$BL \leq \frac{1173}{\delta\lambda^2\frac{dD}{d\lambda}K^{1/2}}\frac{\text{Gb-km}}{\text{s}} \qquad (6)$$

Finally, a different set of performance limits applies to single-mode lasers with very narrow linewidths characterized by $\delta\lambda \leq \lambda^2 B/c$. Within this transform-limited regime, pulse widths become fixed by the modulation speed of the source and $\delta\lambda$ should be replaced by $\lambda^2 B/c$ in equations (3) and (5).

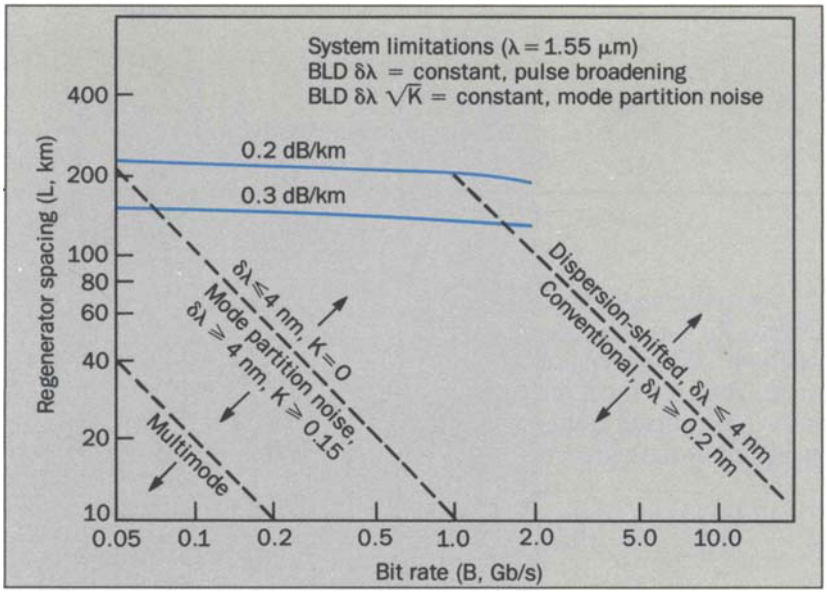

Figure 2. Guide to lightwave systems operating at λ = 1.55 μm.

The maximum separation between repeaters in a lightwave system can be calculated by comparing cable losses (including splices, connectors, etc.) with the differences between the power levels available from optical sources (lasers) and the power levels (including system margin allowances) required for digital reception at various data rates. Present technological limits, for direct detection, are achieved with InGaAs avalanche photodiodes.[7] Their sensitivity is approximately 12 dB higher than the quantum noise limit. Figure 2 plots the achievable repeater spacing (for laboratory experiments at $\lambda = 1.55$ μm without margin allowances) vs. bit rate assuming 0 dBm average power is launched into the fiber from an injection laser and the receiver can detect −43 dBm power (when $B = 420$ Mb/s) at the fiber output. Solid lines indicate performance limitations due to fiber attenuation (0.2 dB/km and 0.3 dB/km). The diagonal lines indicate capacity limitations due to mode partition noise ($K = 0.15$, $\delta\lambda = 4$ nm) and pulse-broadening effects ($K = 0$, $\delta\lambda = 4$ nm and 0.2 nm). The dispersion-shifted performance line ($K = 0$, $\delta\lambda = 4$ nm) assumes that the system wavelength is within 20 nm of the average zero dispersion wavelength along the fiber ($\lambda_o = 1.55 \pm 0.02$ μm).

Parametric Studies

Chromatic dispersion in single-mode fibers is essentially the sum of two effects. The first, material dispersion, is a bulk property which occurs because of the nonlinear dependence of refractive-index on wavelength. It is zero near 1.3 μm for fibers made from lightly doped silica glasses.[8-10] The second effect, waveguide dispersion, occurs because the group velocity of a lightguide mode is also a function of frequency through its dependence on the structure of the waveguide. The key to controlling chromatic dispersion is to use the lightguide structure to tailor the waveguide dispersion spectrum so that it cancels the material dispersion spectrum at one or more wavelengths.[11-13] This can be achieved in step-index fibers with small diameter cores, or equivalently in graded-index fibers with higher maximum indices and larger cores. Computer-aided modeling studies have facilitated choices for such lightguide parameters as the diameter and shape of the refractive-index profile in both the core and the cladding.[14-16]

Lightguides With Silica Cladding

Single-mode lightguide properties can be compared for various graded-index core profile shapes (step,[11] trapezoidal,[17] parabolic, and triangular[18-20]) and SiO_2 cladding (Figure 3a-d) by plotting the wavelength of zero dispersion, λ_o, as a function of:

- Core diameter (Figure 4).
- V number at λ_o normalized relative to the cutoff V value, V_o/V_{co} (Figure 5), where V is the normalized frequency, $V = (\pi dn/\lambda)\sqrt{2\Delta}$, V_{co} is the cutoff demarcation between the single and multimode regimes, and V_o is the normalized frequency at λ_o.
- The effective core-cladding index difference, $\Delta_{eff} = (n_{eff}$

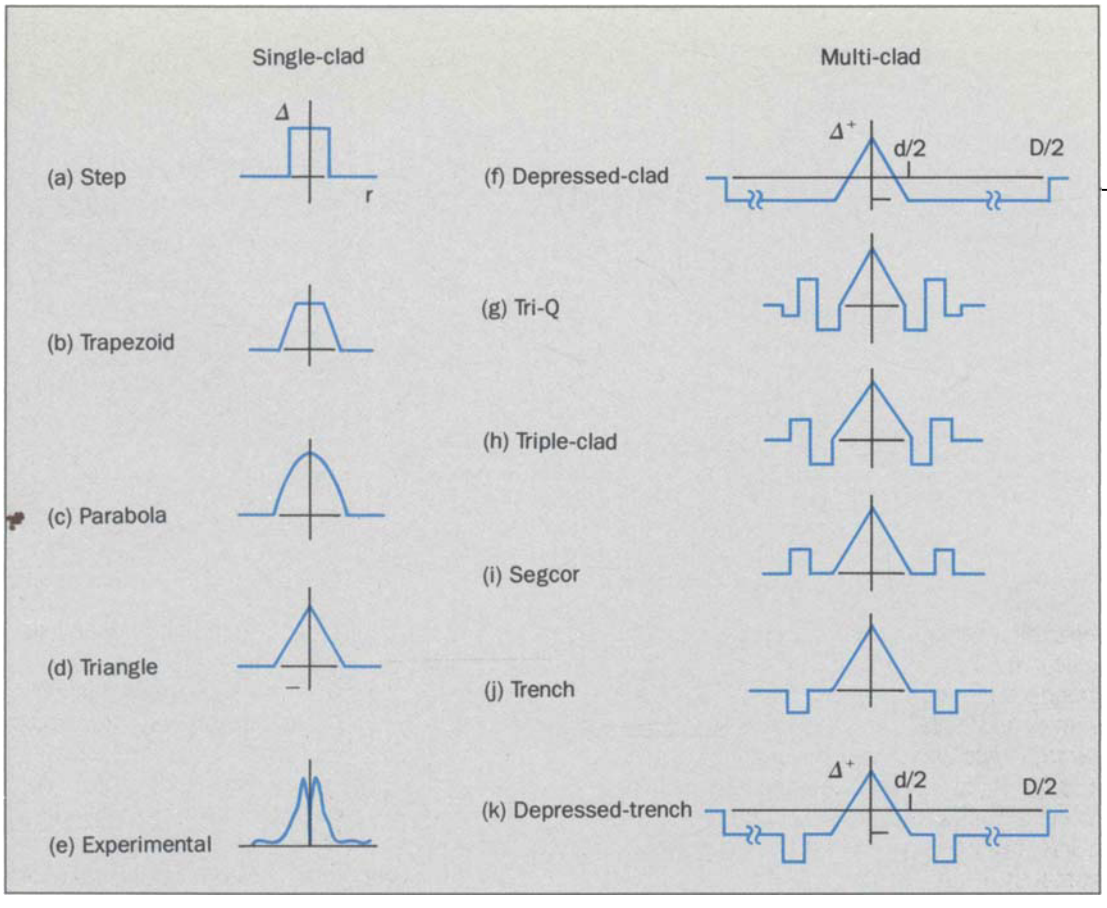

Figure 3. Various index profiles for dispersion-shifted lightguides.

$- n_o)/n_o$, of the fundamental mode (Figure 6), where n_{eff} is the ratio of the modal propagation constant, β, to the propagation constant $k = 2\pi/\lambda$ for a plane wave in free space.[21]

The variable parameter associated with each curve in Figures 4 to 6 is the maximum index difference between the core and the cladding (Δ, in percent).

For the core profiles illustrated, the properties of the step and triangular profiles represent the "extremes" of the variations, with the properties of the parabolic and trapezoidal profiles lying in between. The curves in Figure 4 reach a maxima which minimizes the sensitivity of λ_o to variations of the core diameter. For $\lambda_o = 1.55$ μm, a $\Delta = 0.55$ percent and $d \approx 4$ μm is optimal for a step profile whereas a $\Delta = 0.82$ percent and $d \approx 5.5$ μm is optimal for the triangular profile. From Figure 5 we can then calculate that $\lambda_c^{step} \approx 0.77$ μm and $\lambda_c^{tri} \approx 0.72$ and from Figure 6, $\Delta_{eff}^{step} \approx 0.06$ percent and $\Delta_{eff}^{tri} \approx 0.04$ percent. To demonstrate that the design curves are insensitive to small perturbations, we calculated curves using an experimental triangular profile (Figure 3e). These curves, shown in Figure 7, compare favorably with those in Figures 4d to 6d.

An important observation is that the design curves shown in Figure 5 scale with V_o/V_{co} such that $\lambda_o(\Delta) \approx f(V_o/V_{co})$ for general matched cladding profile shapes. This can be used to derive a general procedure for selecting a set of parameters for any lightguide profile shape. The total chromatic dispersion is the sum of material effects, d_m, which are independent of the lightguide parameters, and waveguide effects, d_w, which can be written in the form

$$d_w = \frac{-L}{2\pi c} V^2 \frac{\partial^2 \beta}{\partial V^2} = \frac{L}{c\lambda} n \Delta D_w(V) \qquad (7)$$

where $D_{w(V)}$ is a dimensionless dispersion coefficient that depends on the V parameter of the fiber.[22] Figure 8 shows $D_{w(V)}$ vs. V for step-index profiles. Its qualitative shape

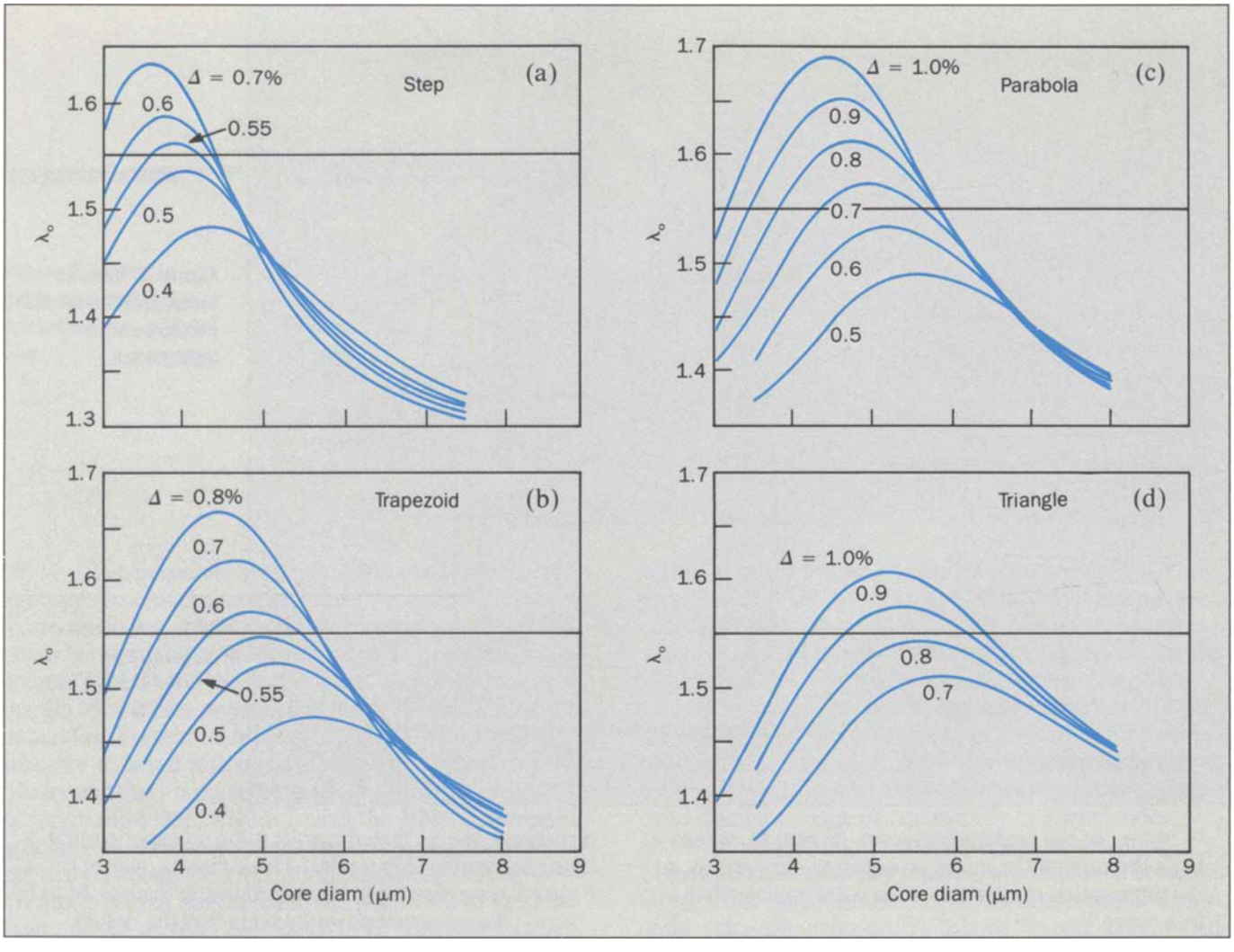

Figure 4. Design guide for λ_o vs. core diameter for step, trapezoidal, parabolic, and triangular profile geometries. For the trapezoidal profile in this figure and in Figures 5 and 6, the ratio of the bases was made 1:2.

depends on $\partial^2\beta/\partial V^2$, which, in turn, depends on the way power is distributed between the core and cladding as a function of V (or λ). For large V (short λ), $D_w \approx 0$ because many modes propagate and the fundamental mode is confined by the core independent of V (or λ). For small V (long λ), $D_w \approx 0$ because mode power is primarily in the cladding. For intermediate values of V ($0.25 < V/V_{co} < 0.5$), $D_{w(V)}$ goes through an extrema because the power distribution, between the core and cladding, changes rapidly as a function of V (or λ).

Since the curves in Figure 5 go through a maximum at $V_o/V_{co} = 0.48$, the peak index-difference, Δ, of the profile may be chosen to minimize the dependence of λ_o on core radius by making the curve tangent to the $\lambda_o = 1.55$ μm line. That defines a minimum $\Delta = \Delta_{min}$ necessary to achieve $\lambda_o = 1.55$ μm. Its value can be calculated approximately by using the waveguide dispersion, defined in equation 7, to cancel the known value of material dispersion, d_m, at any system wavelength (λ_s):

$$\Delta_{min} \approx \frac{c\lambda_s}{nD_w(V = 0.48V_{co})} d_m(\lambda_s) \qquad (8)$$

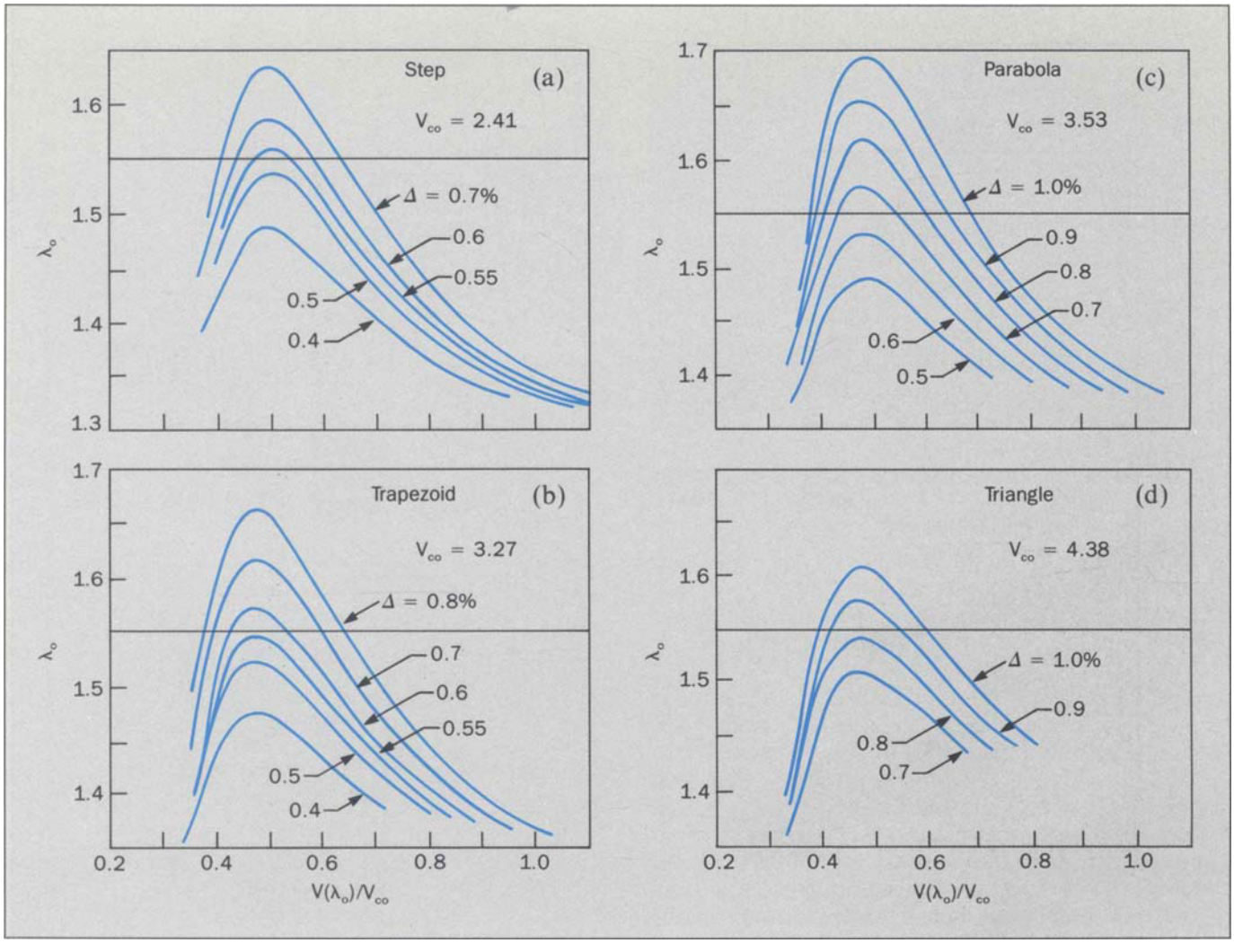

Figure 5. Design guide for λ_o vs. normalized V value $[V(\lambda_o)/V_{co}]$ for step, trapezoidal, parabolic, and triangular profile geometries.

An approximate representation for $d_m(\lambda)$ may be expressed as

$$d_m(\lambda) \approx \frac{S}{4}\lambda\left[\left(\frac{\lambda_{om}}{\lambda}\right)^4 - 1\right] \tag{9}$$

where λ_{om} is the wavelength of zero material dispersion and $S = dd_m/d\lambda|_{\lambda = \lambda_{om}}$ is the slope of the material dispersion spectrum at $\lambda = \lambda_{om}$. Typical values for silica lightguides are[23,24] $\lambda_{om} \approx 1.27$ μm, and $S \approx 0.1$ ps/km-nm^2. After determining Δ_{min}, the corresponding core diameter, d, can be calculated from $V_o/V_{co} \approx 0.48$ by using

$$d = \frac{\lambda_s}{\pi n (2\Delta_{\min})^{1/2}} 0.48\, V_{co} \tag{10}$$

Approximate lightguide parameters can be calculated by relating general matched cladding profile shapes to an equivalent step-index profile as defined by

$$\Delta_{esi} \approx \frac{n_{esi} - n_{cl}}{n_{cl}} \tag{11a}$$

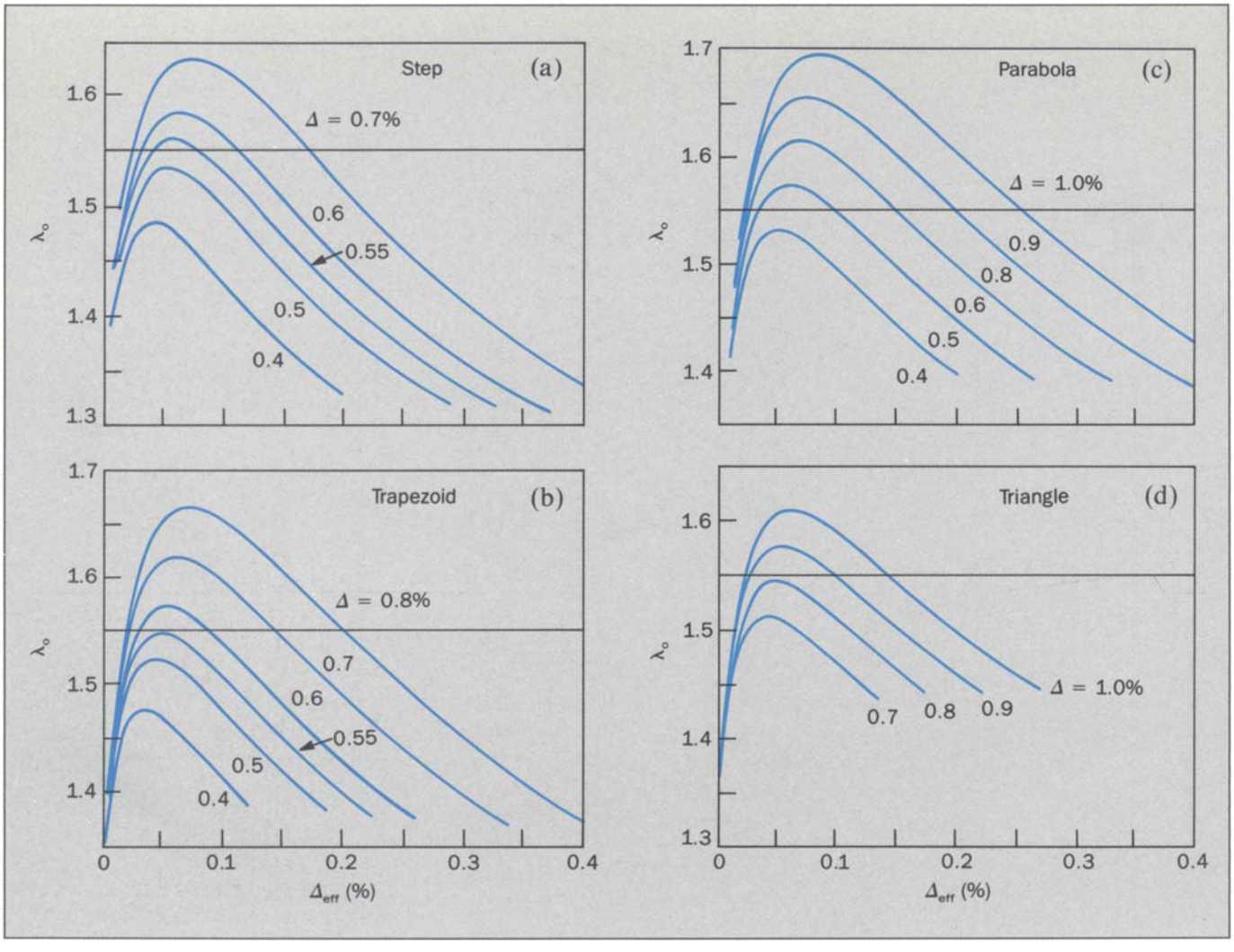

Figure 6. Design guide for λ_o vs. effective index (Δ_{eff}) for step, trapezoidal, parabolic, and triangular profile geometries.

$$\Delta_{esi} = \frac{1}{n_{cl}^2}\int_0^1 (n_{core}^2(\bar{r}) - n_{cl}^2)\,\bar{r}d\bar{r}$$
$$= \frac{1}{n_{cl}^2}\int_0^1 (n_{esi}^2(\bar{r}) - n_{cl}^2)\,\bar{r}d\bar{r} \qquad (11b)$$

where $n_{core}(\bar{r})$ defines a normalized profile as a function of $\bar{r} = r/a$. For example, a power-law profile may be defined by the following equation:

$$n_{cl} = n_o(1 - 2\Delta\,\bar{r}^{\alpha})^{1/2}; \quad n_{cl} = n_o(1 - 2\Delta)^{1/2} \qquad (12)$$

so that a linearly graded triangular index profile is characterized by $\alpha = 1$ and, from equation (11), $\Delta_{esi} = (\Delta_{tri}/3)^{1/2}$. Using equation (10), a core diameter of 5.2 μm is calculated which agrees with the data in Figure 4. The procedure outlined above is consistent with the data calculated by using computer-modeling programs and the various profile shapes (Figures 4 to 6).

Although it is desirable to minimize the dependence of λ_o on core radius, often other requirements lead to slight design modifications. For example, for the triangular core profile Figure 4d shows that a design curve for $\Delta \approx$

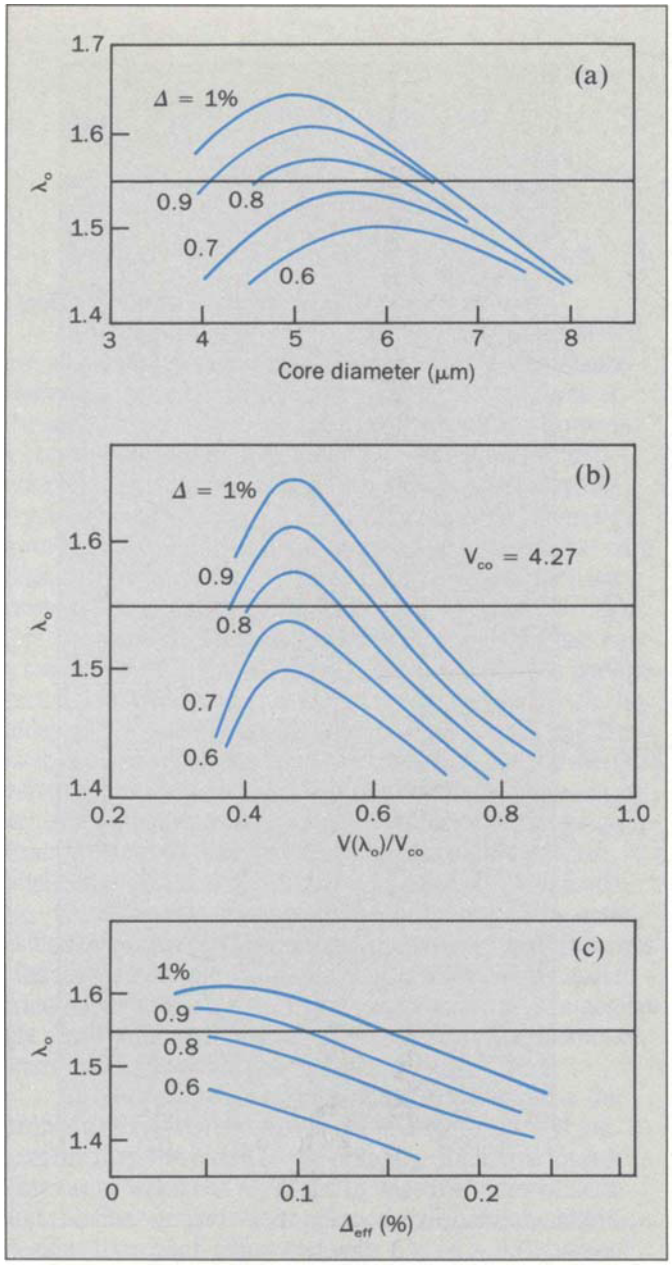

Figure 7. Design guides calculated from measured index profiles with triangular cores.

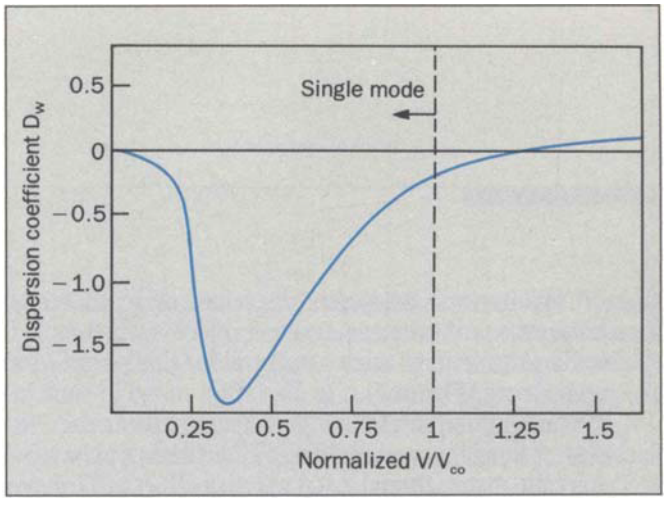

Figure 8. Waveguide dispersion coefficient[22] D_w vs. V/V_{co}.

0.82 percent would have a maximum $\lambda_o = 1.55$ μm at $d \approx 5.5$ μm. However, in order to ensure low intrinsic bending losses, tight mode confinement must be maintained by keeping Δ_{eff} and V/V_{co} as large as possible at $\lambda_o \approx 1.55$ μm.[25] A place to the right of the design curve maximum may be selected for a slightly higher Δ (0.9 percent $< \Delta < 1.0$ percent) corresponding to a core diameter $6 < d < 6.5$ μm, a V value between $0.6 < V_o/V_{co} < 0.65$, and an effective index between 0.1 percent $< \Delta_{eff} < 0.15$ percent. The increased sensitivity of the design to core diameter variations is more than compensated by the improvement in microbending loss.

The triangular core lightguide structure has been the most successful for achieving low losses with dispersion shifting.[18-20] The linear gradient profile forms a self-focusing guide which confines the propagating beam to a smaller spot inside the core than the other profile geometries. Since dispersion-shifted fibers require large waveguide dispersion at the longer wavelengths and waveguide dispersion becomes larger as the spot size becomes smaller, it is clear that a triangular graded-index lightguide can have a larger core diameter than a step-index fiber and still produce the same magnitude of waveguide dispersion. The triangular structure also provides the added benefits of a smoother and less abrupt interface between the cladding and the higher-index core region and a tolerance to wider deviations of core diameters than than the step-index guide. An abrupt interface between the core and the cladding (e.g., step-index fiber) has been associated in practice with higher loss.[19] Dispersion-shifted lightguide characteristics of triangular core guides are also reasonably tolerant to small variations in the refractive-index profile

shape.[26] The transmission properties have been calculated from triangular profiles measured on preforms which exhibited imperfections, such as central-index dips and disjointed slopes (Figure 7).

Another important lightguide parameter is the thickness of the deposited cladding. The cladding (deposited plus tube material) makes up approximately 99.7 percent of the total fiber volume (e.g., core diameter $\approx$ 7 μm, fiber diameter = 125 μm). Preform processing times can be significantly reduced by minimizing the volume of cladding glass deposited within a thick tube of a lower optical grade.

However, if the cladding to core ratio, D/d, becomes too small, then fiber losses will increase either from light penetration into the lossy substrate tube, or from leaky-mode effects when the refractive index of the deposited cladding is depressed below the index of the surrounding substrate tube.

Loss from the first mechanism occurs when the mode power distribution, P, extends beyond the deposited cladding and a fraction of the propagating light travels in the lossy material of the substrate tube. Losses from leaky-mode effects occur in depressed cladding designs when the effective index of the fundamental mode becomes less than the index of the substrate tube and the mode power distribution extends into the deposited cladding. The mode is then no longer strictly guided and power is radiated into the cladding.

The guided mode power decreases with an approximately Gaussian dependence on r/a within the core but then changes to a slower exponential dependence for $r/a > 2$. Figure 9 generalizes these results by plotting the D/d required to keep the fractional power

$$\bar{P}_s = \frac{P_{substrate}}{P_{total}} \qquad (13)$$

less than some specific value as a function of V/V_{co} for several profile shapes.[21,27] This criterion for $\bar{P}_s$ was chosen to keep added losses below 0.01 dB/km due to power penetration into a substrate region which has an assumed loss of 100 dB/km.

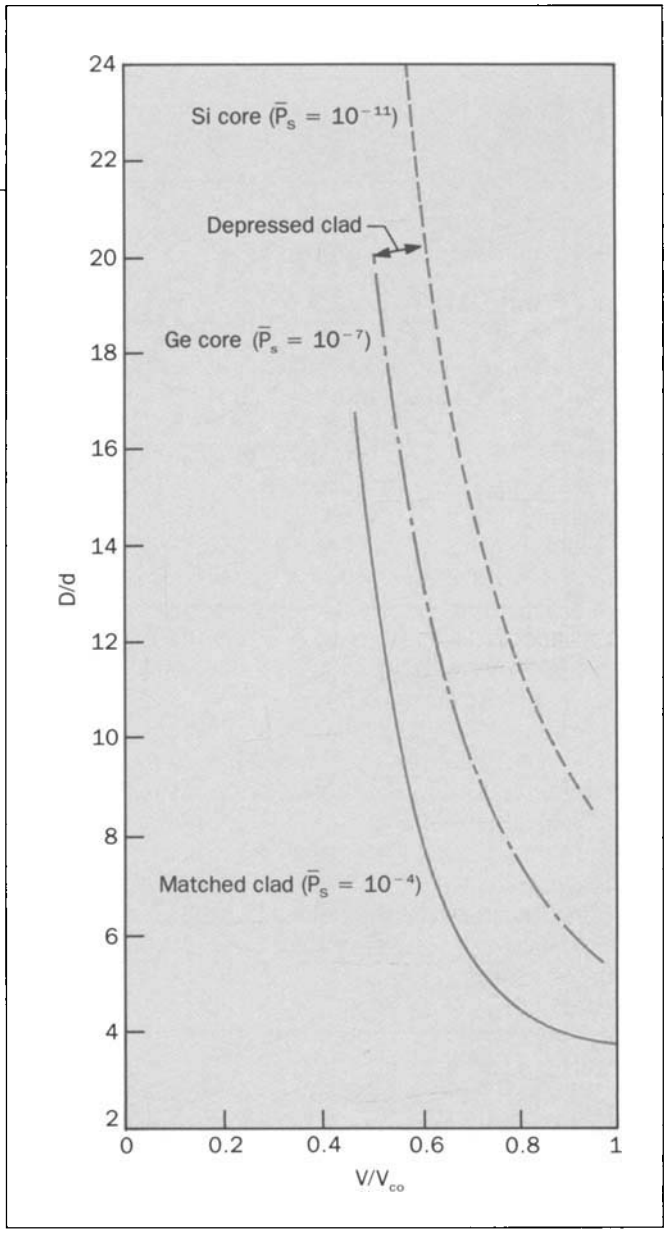

Figure 9. D/d vs. V/V_{co} limitations for matched-clad, depressed-clad, and silica core profiles.[27]

For example, the requirement that $V/V_{co} \approx 0.6$ for dispersion-shifted lightguides (Figure 5) constrains the clad-to-core diameter ratio to be $D/d > 7$.

Lightguides with Depressed-Index Outer Claddings

The profile geometries that have been discussed are all examples of matched cladding structures because the refractive index of the outer cladding is the same as the index of the substrate tube (typically SiO_2). However, intrinsic fiber losses are limited by Rayleigh scattering effects which depend on the core dopant concentration (typically germania) and the cladding material. Therefore, lower intrinsic losses can be achieved by lowering the core dopant concentration and using fluorine as a dopant to depress the cladding indices below silica in order to maintain the same Δ. This material modification will have only a minor effect on the previously derived lightguide parameters if a fluorosilicate substrate tube is used to match the index of the outer deposited fluorosilicate cladding.[27] However, if silica substrate tubes are used (the norm), then the constraint on D/d changes because additional losses may occur if a significant fraction of the total power leaks away from the core as it propagates along the lightguide axis.[21] Such losses occur when the effective index of the mode, $n_{eff} = \beta/k$, becomes less than the index, n_o, of the outer cladding. However, this does not presuppose high transmission losses because the deposited cladding can be made wide enough to allow the mode power to decay to a negligibly small value at the outer diameter, D, of the index well from which the mode power leaks.

For small depressions of the cladding index the problem of radiative losses is not as severe since n_{eff} is greater than the index of the cladding. Radiative losses only occur when the n_{eff} drops to near the index of silica and the fiber is bent. Triangular core dispersion-shifted designs have been fabricated with $\Delta^- \approx -0.12$ percent which have consistently yielded losses at $\lambda = 1.55$ μm less than those of the matched cladding design[24] (see Figure 3f). Since the $\Delta_{eff} \approx 0.1$ percent ($\Delta = 0.9$ percent) at 1.55 μm, radiative losses become a problem when $\Delta^- < -0.2$ percent and D/d must be increased.

The procedures described in Reference 21 can be used to calculate macrobending losses as a function of curvature by approximating depressed-index cladding lightguides with equivalent step-index core profiles. Figure 9 plots D/d vs. V/V_{co} requirements that are necessary to prevent macrobending effects from becoming significant because of bends with radii of curvature larger than 7.5 cm. As an example, dispersion-shifted lightguides ($V/V_{co} \approx 0.6$), with a totally depressed-index cladding ($\Delta^+ = 0$), require $D/d \approx 24$ in order to maintain

$$\bar{P} = \frac{P_{substrate}}{P_{total}} < 10^{-11} \qquad (14)$$

which is necessary to keep additional losses < 0.01 dB/km at $\lambda \approx 1.55$ μm. This is significantly larger than the $D/d \approx 10$ requirement for silica-core fibers without dispersion-shifting ($V/V_{co} \approx 0.8$).[28]

Strategies to reduce the required deposited cladding thickness are of interest since they can reduce the fabrication time (and thus the cost) of the manufactured fiber. For depressed cladding structures, the constraint of leaky-mode effects can be removed by producing fluorosilicate substrate tubes to match the index of the outer deposited cladding.[26] For slightly depressed and matched cladding structures the mode power at the interface separating the depressed-index cladding from the substrate can be reduced by adding a depressed index ring or trench around the core at a relatively large distance from the core (see "Reduced Cladding Power" below).

Lightguides with Multiple Deposited Claddings

One disadvantage of single-clad dispersion-shifted fibers is that they are usually low V-value lightguides with cutoff wavelengths that are considerably shorter than 1.55 μm. Because a significant fraction of the propagating modal power is distributed within the cladding, fiber losses may increase due to macro- and microbending effects which occur if the fiber is wrapped around a drum or packaged within a cable. An attractive feature of multi-clad structures is that the core and inner cladding can be designed to control dispersion spectra and the remaining

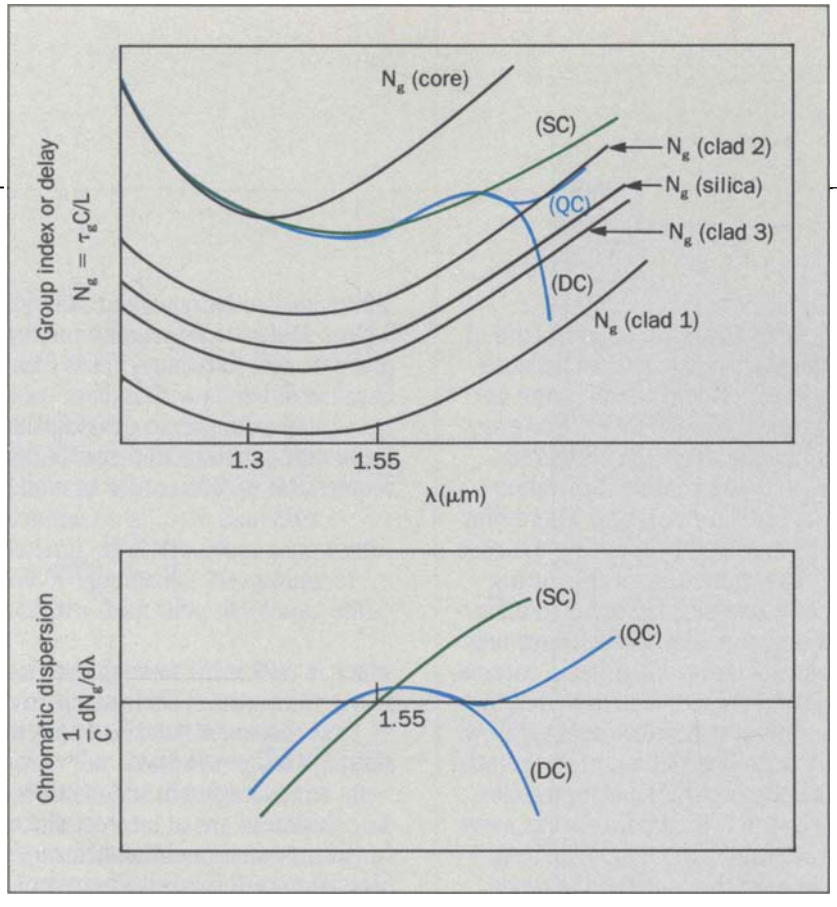

Figure 10. Evolution of group index, N_g, and dispersion for a quadruple-clad (QC) index profile. Comparisons are made with respect to single-clad (SC) and double-clad (DC) profiles.

Figure 11. λ_o vs. core diameter for trench profile shown in (a) as a function of Δ^+ for (b) t/a = 1.5, (c) t/a = 3.5.

claddings can be independently tailored to improve mode confinement and reduce bending-related losses.

A structure consisting of suitably designed claddings with raised indices and suppressed wells surrounding the core can be used to independently control the dispersion spectra and mode-confinement properties. Several multi-clad structures are illustrated in Figure 3 and others have been described in the literature.[13,29-33] The triple-clad profile structure (Figure 3h) is typical of a multiply clad, dispersion-shifted fiber.[29,31] The triangular core is used to shift the dispersion zero to 1.55 μm and the raised outer ring increases the cutoff wavelength for better mode confinement. Fibers with this design have been used to achieve λ_o = 1.55 μm and low losses (0.21 dB/km).[31]

The quadruple-clad profile structure (Figure 3g) was first used to demonstrate the advantages of multiple-index deposited claddings, and a fiber with this design was the first to achieve less than 2 ps/km-nm dispersion over an ultra-broad wavelength range spanning the 1.28 μm to 1.65 μm region.[13] The Q fiber is characterized by eight parameters ($\Delta(i)$, $R(i)$, i = 1,4) that can be varied to optimize loss and dispersion properties. In general, parameters relating to the core and first cladding are used to flatten the dispersion spectra while the remaining parameters are used to maintain low losses. The function of the various cladding regions can be understood by referring to Figure 10 which plots the group-index (solid line) of the propagating mode versus λ. The dotted curves show the material group-index spectra (N_g) for the materials of the core and four claddings (n_{core}, n_i, i = 1,4). At short wavelengths, the mode is confined to the core and N_g is asymptotic to the core index. At longer wavelengths, the mode power penetrates into cladding 1 which decreases N_g toward n_1. The mode would become unguided (cut off) if N_g were to become less than the index, n, of the outer silica cladding such as for the curve labeled DC. However, at wavelengths where that could happen, the mode penetrates into the second cladding which has a raised index

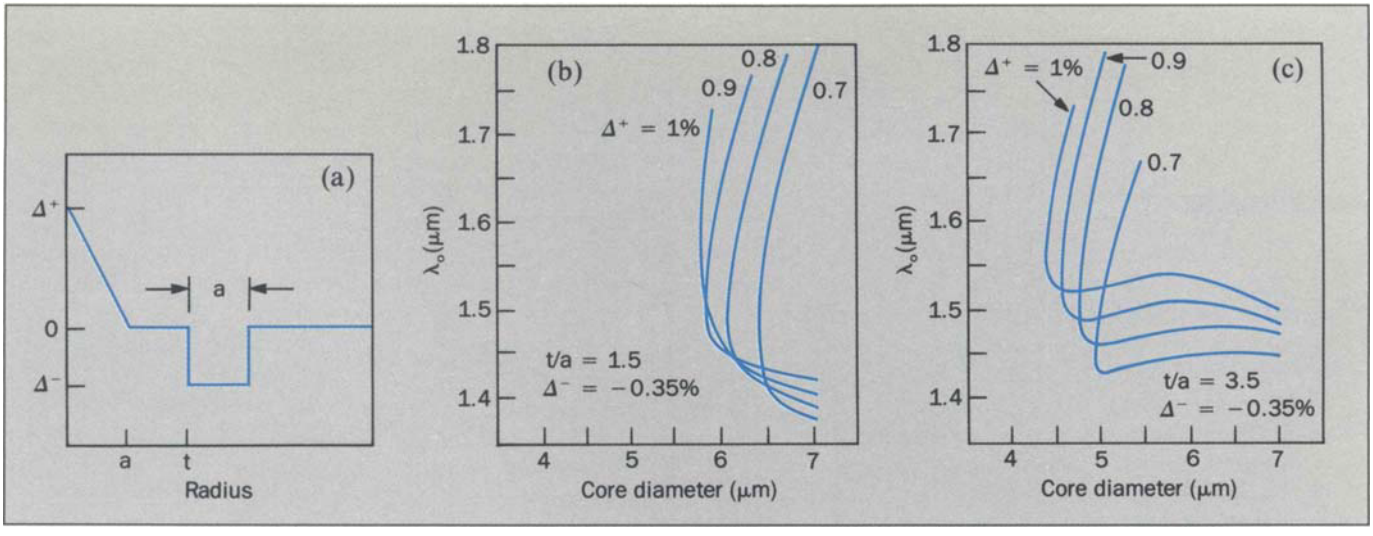

with a peak value of n_2. This annular ring region forms a secondary lightguide that can retrap light which would otherwise radiate away from the core due to axial bending effects. As a result, N_g increases towards n_2 which prevents the fundamental mode from becoming cut off. At still longer wavelengths N_g decreases towards n_3 and finally becomes asymptotic to n_4, the index of the outermost cladding (usually silica). The third cladding n_3 forms a depressed-index well which is used to ensure single-mode operation and reduce the extent of power penetration in the outermost cladding. Since chromatic dispersion is obtained by differentiating the delay with respect to wavelength, the resultant dispersion spectra can be flattened because $dN_g/d\lambda$ can have three extrema corresponding to three wavelengths of zero dispersion.

The Trench Fiber

Figure 3j illustrates a new lightguide structure which uses a depressed-index ring or trench placed around the core. Depending upon the placement, width and depth of the trench, the λ_o may be adjusted, the power in the mode at radii larger than the trench may be reduced, and, as also shown by T. A. Lenahan of AT&T Bell Laboratories, the slope of the dispersion spectra may be decreased.

Controlling Dispersion. For the trench to be effective in controlling the dispersion of a fiber it must be placed within several core radii of the fiber center. Figures 11b and c illustrate the dependence of λ_o on core diameter for a triangular core fiber with a trench one core radius wide and $\Delta^- = -0.35$ percent deep placed 1.5 and 3.5 core radii away from the fiber center (Figure 11a). The parameter associated with each curve is the Δ^+ of the core. Dispersion spectra are flattened within the regions of Figures 11b,c where there are two values of λ_o for a fixed core radius. For $t/a = 1.5$ the trench affects the dispersion for $d < 6.5$ μm, whereas for $t/a = 3.5$ the shape of the lower branches of the dispersion spectra are essentially unchanged. However, the value of λ_o for each Δ^+ is less than the λ_o for similar curves shown in Figure 4d for $d > 5$ μm. For intermediate values of t/a the trench reduces both λ_o and the dispersion slope. The evolution of λ_o for t/a between 1 and 3.5 is shown in Figure 12 for $\Delta^+ = 0.9$ percent. The influence of the trench on dispersion in this case becomes negligible for $t/a > 6$.

Figure 13a shows dispersion spectra corresponding to Figure 11a with $\Delta^+ = 0.9$ percent and different core diameters. As the core diameter is reduced, power extends further into the cladding, and the trench influences dispersion at shorter wavelengths. The effect is to displace dispersion spectra downward and move the two zero-dispersion wavelengths closer together until the chromatic-dispersion curve becomes tangent to the zero dispersion axis. For even smaller diameters the chromatic-dispersion curves move completely below the zero axis. For comparison, Figure 13b shows the dispersion spectra for the same index profile as for Figure 13a but without the trench.

Figure 14 illustrates one way the addition of a trench can reduce the dispersion slope. Profile (a) has a triangular core and a raised index ring whereas profile (b) is the same as (a) except that a trench has been added just outside the ring. As we discussed in regard to Figure 10,

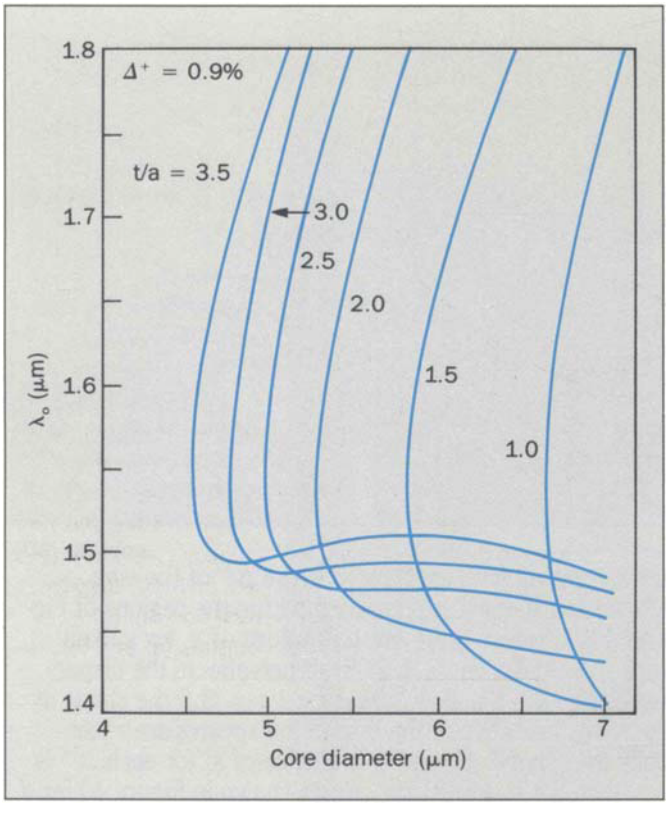

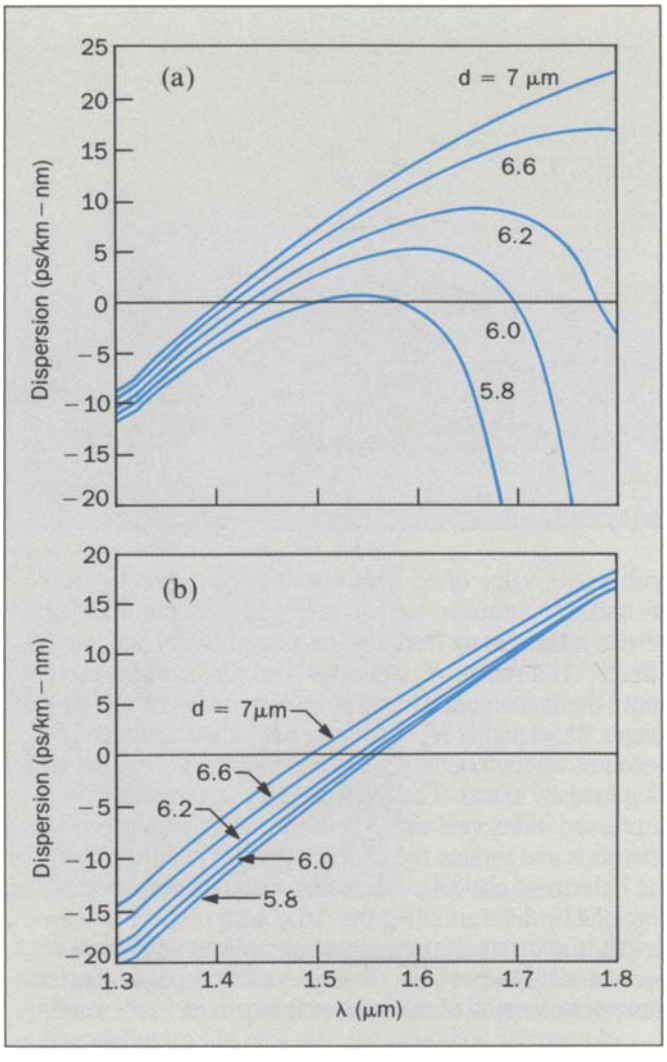

Figure 12. λ_o vs. core diameter for trench profile in Figure 11a as a function of *t/a* for $\Delta^+ = 0.90$ and $\Delta^- = -0.35$.

Figure 13. Dispersion vs. λ as a function of core diameter for (a) trench profile (Figure 11a), $\Delta^+ = 0.90$, $\Delta^- = -0.35$, and *t/a* = 1.5, (b) triangular profile without trench, $\Delta^+ = 0.90$.

the group index increases as the mode spreads into the region of the ring and then asymptotically approaches the group index of the silica outer cladding. The addition of the trench outside the ring causes the group index to decrease more rapidly which decreases the slope of the dispersion. For both profiles $\lambda_o = 1.56$ μm at a core diameter of 5.5 μm. It is interesting to note that the ring, like the trench at small *t/a*, decreases the λ_o for the same Δ^+ and core size. The same core profile ($\Delta^+ = 1.1$ percent) without the ring (which we will call m1) has a $\lambda_o = 1.62$ μm at $d = 5.5$ μm, whereas $\lambda_o = 1.56$ μm at $d = 6.2$ μm. To achieve $\lambda_o = 1.56$ μm at $d = 5.5$ μm, $\Delta^+ = 0.85$ percent is required (which we will call m2). The integrated power for profiles (a), (b), and two profiles without the ring or trench (m1, m2) are plotted in Figure 14c. The larger Δ^+ of profile m1 provides better power confinement than profile m2 but will have greater Rayleigh scattering. The addition of the ring decreases the power confinement for the same Δ^+ and the addition of the trench beyond the ring slightly improves the power confinement compared to the ring alone. However, a more important effect of the trench is to reduce the slope of the dispersion spectra at λ_o (Figure 14d). The trench reduces the slope from 0.089 ps/km-nm^2 for curve (a) to 0.074 ps/km-nm^2 for curve (b). These slopes can be compared to 0.078 ps/km-nm^2 for profile m2 and 0.063 ps/km-nm^2 for profile m1. Adding the trench provides a 17 percent improvement in the slope compared to the profile with only the ring.

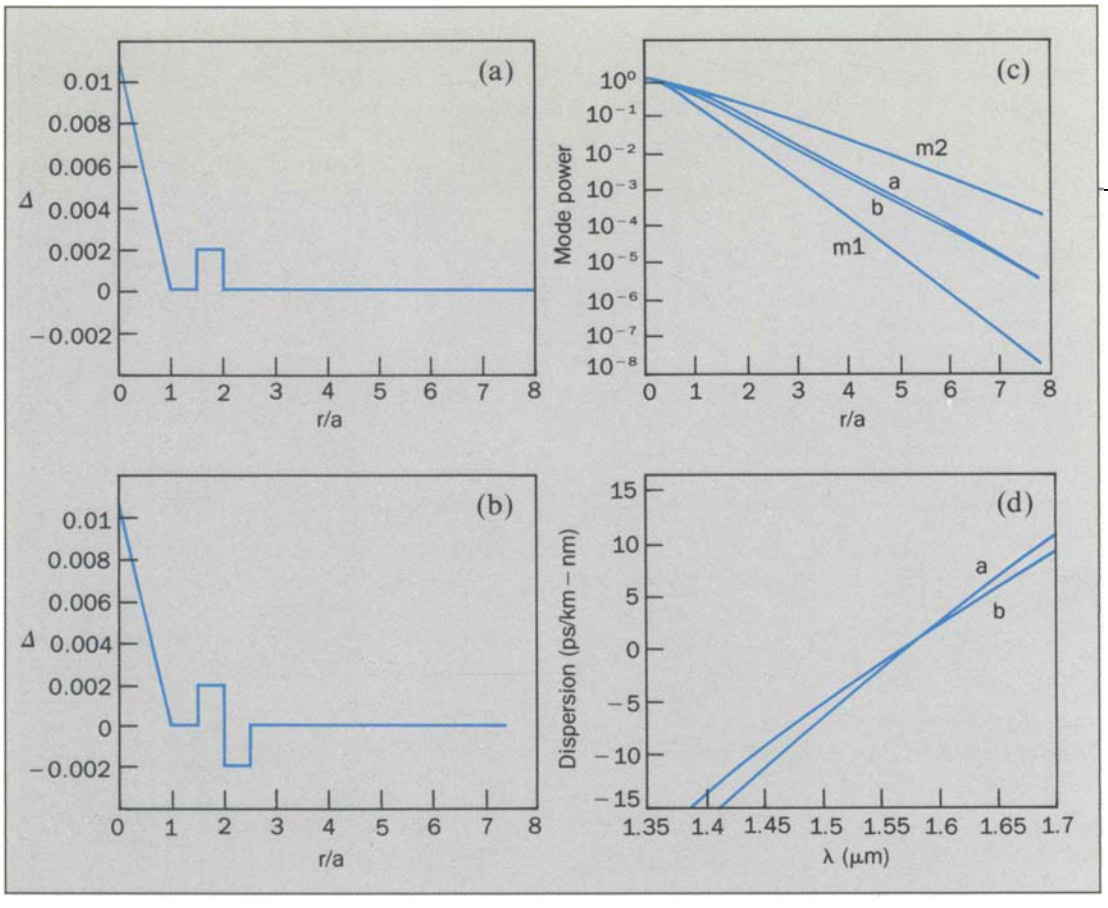

Figure 14. Index profiles for a triangular core with (a) raised-index ring and (b) raised index-ring with trench. Integrated mode power (c) for these profiles and two matched clad profiles m1 and m2. Dispersion spectra (d) for profiles (a) and (b).

Reducing Cladding Power. Another property of the depressed-index ring or trench design is that the mode power decreases in the region of the trench and remains less than the mode power for a similar fiber design without the trench. By placing the trench several core radii away from the core, the dispersion properties of the guide are essentially unchanged whereas the mode power confinement is improved. Figures 15a-c illustrate several lightguide profiles which demonstrate this use of the trench. Each has a triangular profile with a central index depression ($\Delta^+ = 0.8$ percent) in the core. However, significant differences occur in the cladding. In Figure 15a the cladding is depressed ($\Delta^- = -0.2$ percent) out to $r/a = 8$ for profile a1 and out to $r/a = 10$ for profile a2. In Figures 15b,c the profile is the same as a1 except that a trench with a total depth of $\Delta^- = -0.4$ percent and a width of two and three core radii, respectively, is placed at the outer edge of the depressed cladding. In these examples the trenches are far enough from the core so that they shift λ_o less than 0.002 μm compared to λ_o for profile a1 or profile a2.

Figure 15d plots the integrated mode power vs. radius at $\lambda = 1.55$ μm and a core diameter of 5.5 μm for each profile. These indicate that the power roll-off is approximately Gaussian ($\approx e^{-r^2}$) for small radii and exponential ($\approx e^{-r}$) for large radii. Notice that the trench reduces the amount of power that can extend beyond its confines. We calculate that $V(\lambda_o)/V_{co} = 0.65$ for profile a2 so that from Figure 9 we find that a D/d of 10 is required for $\bar{P} < 10^{-7}$ which is necessary to minimize bend losses. Thus from Figure 15d we see that profile a1 has too small a D/d since $\bar{P} = 10^{-7}$ at $r/a \approx 10.5$ whereas profile a2 with $D/d = 10$ is satisfactory, as expected from Figure 9. Notice however, that $\bar{P}$ for both profiles (b) and (c) reach the 10^{-7} level at $r/a \approx 8$ and 7 respectively. Thus better power confinement is achieved with a trench and the $D/d = 8$ represents a 20 percent savings in deposited cladding compared to profile a2.

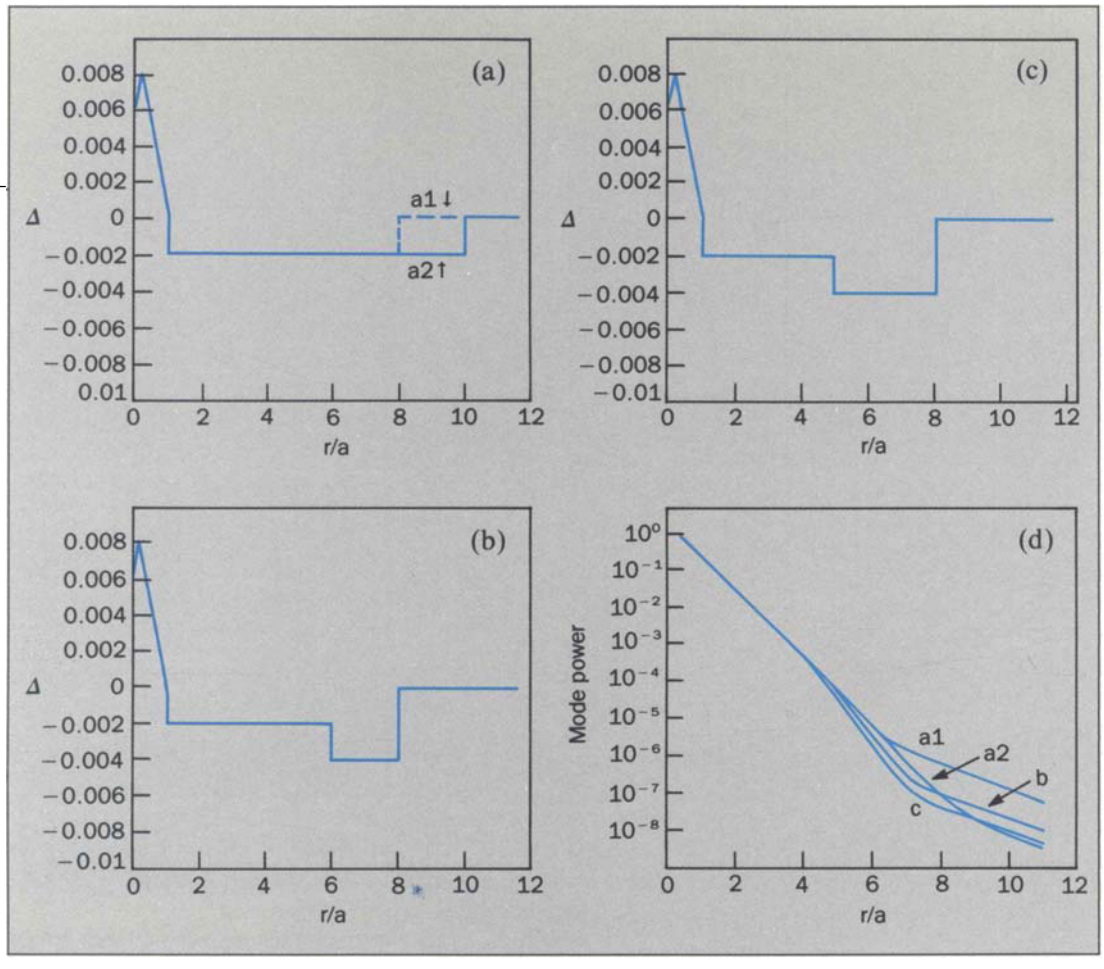

Figure 15. Index profiles with and without trench and related integrated mode power.

Conclusions

This paper describes the propagation characteristics of fibers with low dispersion near 1.55 μm. Systems operated at 1 Gb/s over 210 km in conventional fiber become dispersion-limited (at $\lambda_s = 1.55$ μm) if the laser spectral width is greater than 0.2 nm. By comparison dispersion-shifted fibers, with less than 1 ps/km-nm dispersion and a loss of 0.2 dB/km, could support transmission over longer lengths even if the laser spectral width increased to 4 nm.

Computer-aided modeling studies have been used to understand propagation characteristics and choose parameters for various dispersion-shifted fiber designs. They include curves of modal power radial profiles and tolerance curves for the zero dispersion crossover wavelength as a function of core index and dimensional parameters. Propagation characteristics have been modeled for lightguides that include matched-cladding, multiple-cladding, and depressed-cladding designs.

Graded-core lightguides with triangular, parabolic, and trapezoidal profile shapes have been analyzed. Parametric design curves are used to study how lightguide parameters affect dispersion and mode confinement near $\lambda_o = 1.55$ μm. The curves all have single extrema at 0.48 when plotted vs. V/V_{co}. Therefore, fiber core diameter and core-clad index differences can be chosen to minimize tolerance requirements by making the maximum point of the design curves correspond to $\lambda_o = 1.55$ μm. However, the need to minimize extrinsic bending effects makes it imperative to optimize mode confinement characteristics by choosing V_o/V_{co} and Δ_{eff} as large as possible. For the triangular core design plots of λ_o vs. V_o/V_{co} and Δ_{eff} were used to identify the region to the right of the design peak, corresponding to 0.8 percent $< \Delta <$ 1.0 percent, as the best

choice ($0.45 < V_o/V_{co} < 0.60$; 0.05 percent $< \Delta_{eff} <$ 0.15 percent). Curves for mode power confinement vs. radius were then used to determine the thickness of deposited cladding ($D/d \approx 8$) required to isolate the lossy substrate cladding from the lightguide region.

Since dispersion-shifted lightguides have relatively small V/V_{co}, they therefore require thick deposited claddings to prevent a significant fraction of the total power from either traveling in the high-loss substrate cladding or leaking through the substrate cladding at the interface with the depressed-index cladding region. Quantitative requirements are illustrated for D/d vs. V/V_{co}. As an example, silica core lightguides with triangular graded-index profiles require a $D/d \approx 24$ in order to keep the fractional leaky-mode power low enough ($P < 10^{-11}$) to ensure that macrobending losses remain less than 0.01 dB/km at $\lambda \approx 1.55$ μm.

Lightguides with multiple deposited claddings can be used to independently control dispersion spectra and mode-confinement properties. A novel and relatively simple profile modification was proposed to have a depressed-index ring or trench surrounding the core at a relatively large distance from the core. The diameter, width, and depth of the trench can be adjusted to flatten dispersion spectra or relax requirements on D/d by reducing the amount of power at the lossy substrate cladding by about two orders of magnitude. One example illustrates how a trench can reduce the required deposited cladding by 20 percent.

References

1. K. Ogawa, "Considerations for Single-Mode Fiber Systems," *Bell System Technical Journal*, Vol. 61, No. 8, October 1982, pp. 1919-1931.
2. L. G. Cohen et al., "Transmission Studies of a Long Single-Mode Fiber—Measurements and Considerations for Bandwidth Optimization," *Bell System Technical Journal*, Vol. 60, No. 8, October 1981, pp. 1713-1725.
3. F. P. Kapron, "Maximum Information Capacity of Fiber-Optic Waveguides," *Electronics Letters*, Vol. 13, 1977, pp. 96-97.
4. L. G. Cohen, W. L. Mammel, and S. Lumish, "Dispersion and Bandwidth Spectra in Single-Mode Fibers," *IEEE Journal of Quantum Electronics*, Vol. QE-18, 1982, pp. 49-53.
5. K. Ogawa, "Analysis of Mode Partitioning Noise for Laser Diode System," *IEEE Journal of Quantum Electronics*, Vol. QE-17, 1982, pp. 849-855.
6. R. A. Linke, "Transient Chirping in Single-Frequency Lasers: Lightwave Systems Considerations," *Electronics Letters*, Vol. 20, 1984, pp. 472-474.
7. J. C. Campbell et al., "High Performance Avalanche Photodiode with Separate Absorption, Grading, and Multiplication Regions," *Electronics Letters*, Vol. 19, 1983, pp. 818-820.
8. L. G. Cohen and C. Lin, "Pulse Delay Measurements in the Zero Material Dispersion Wavelength Region for Optical Fibers," *Applied Optics*, Vol. 16, 1977, pp. 3136-3139.
9. P. D. Lazay and A. D. Pearson, "Developments in Single-Mode Fiber Design, Materials and Performance at Bell Laboratories," *IEEE Journal of Quantum Electronics*, Vol. QE-18, 1982, pp. 504-510.
10. W. M. Flegal et al., "Mass Production of Depressed Clad Single-Mode Fiber," Conference on Optical Fiber Communications (OFC '84), January 23-25, 1984, New Orleans, *Technical Digest*, pp. 56-57.
11. L. G. Cohen, C. Lin, and W. G. French, "Tailoring Zero Chromatic Dispersion in the 1.5-1.6 μm Low-Loss Spectral Region of Single-Mode Fibers," *Electronics Letters*, Vol. 15, 1979, pp. 334-335.
12. L. G. Cohen, W. L. Mammel, and S. Lumish, "Tailoring the Shapes of Dispersion Spectra to Control Bandwidths in Single-Mode Fibers," *Optics Letters*, Vol. 7, 1982, pp. 183-185.
13. L. G. Cohen, W. L. Mammel, and S. J. Jang, "Low-Loss Quadruple-Clad Single-Mode Lightguides with Dispersion Below 2 ps/km-nm over the 1.28 μm-1.65 μm Wavelength Range," *Electronics Letters*, Vol. 18, 1982, pp. 1023-1024.
14. L. G. Cohen, W. L. Mammel and H. M. Presby, "Correlations Between Numerical Predictions and Measurements of Single-Mode Fiber Dispersion Characteristics," *Applied Optics*, Vol. 19, 1980, pp. 2007-2010.
15. W. L. Mammel and L. G. Cohen, "Numerical Prediction of Fiber Transmission Characteristics from Arbitrary Refractive-Index Profiles," *Applied Optics*, Vol. 21, pp. 699-703.
16. T. A. Lenahan, "Calculation of Modes in an Optical Fiber Using the Finite Element Method and Eispack," *Bell System Technical Journal*, Vol. 62, No. 9, November 1983, pp. 2663-2694.
17. T. J. Miller and D. H. Smithgall, "Fabrication of Trapezoidal-Index Profile Single-Mode Fiber," Conference on Optical Fiber Communications (OFC '84), January 23-25, 1984, New Orleans, *Technical Digest*, pp. 54-55.
18. M. A. Saifi et al., "Triangular-Profile Single-Mode Fiber," *Optics Letters*, Vol. 7, 1982, pp. 43-45.

19. B. J. Ainslie et al., "Monomode Fibre with Ultra-Low Loss and Minimum Dispersion at 1.55 μm," *Electronics Letters*, Vol. 18, 1982, pp. 842-843.
20. A. D. Pearson et al., "Optical Transmission in Dispersion-Shifted Single-Mode Spliced Fibers and Cables," *Journal of Lightwave Technology*, Vol. LT-2, 1984, pp. 346-349.
21. L. G. Cohen, D. Marcuse, and W. L. Mammel, "Radiating Leaky-Mode Losses in Single-Mode Lightguides with Depressed-Index Claddings," *IEEE Journal of Quantum Electronics*, Vol. QE-18, 1982, pp. 1467-1472.
22. D. Gloge et al., *Optical Fiber Telecommunications* (S. E. Miller and A. G. Chynoweth, eds.), Academic Press, New York, 1979, p. 105.
23. J. W. Fleming, "Material Dispersion in Lightguide Glasses," *Electronics Letters*, Vol. 14, 1978, pp. 326-328.
24. H. T. Shang et al., "Dispersion-shifted Depressed-clad Triangular-profile Single-mode Fiber," Conference on Optical Fiber Commununications (OFC '85), February 11-13, 1985, San Diego, *Technical Digest*, pp. 93-93.
25. S. J. Jang et al., "Fundamental Mode Size and Bend Sensitivity of Graded and Step-Index Single-Mode Fibers with Zero-Dispersion Near 1.55 μm," *Journal of Lightwave Technology*, Vol. 3, 1984, pp. 312-316.
26. B. J. Ainslie et al., "Transmission Properties of Triangular Profile Monomode Fiber for 1.55 μm Operation," Fourth International Conference on Integrated Optics and Optical Fiber Communication (IOOC '83), June 27-30, 1983, Tokyo, *Technical Digest*, pp. 46-47.
27. J. B. MacChesney et al., "Fluorosilicate Substrate Tubes to Eliminate Leaky-Mode Losses in Single-Mode Fiber with Depressed Index Cladding," *Journal of Lightwave Technology*, Vol. LT-3, 1984, pp. 942-945.
28. K. Ciemiecki Nelson et al., "Fabrication and Performance of Long Lengths of Silica Core Fiber," Conference on Optical Fiber Communication (OFC '85), February 11-13, 1985, San Diego, *Technical Digest*, pp. 98-99.
29. S. J. Jang et al., "Graded-Index Single-Mode Fibers with Multiple Claddings," Fourth International Conference on Integrated Optics and Optical Fiber Communication (IOOC '83), June 27-30, 1983, Tokyo, *Technical Digest*, pp. 396-397.
30. V. A. Bhagavatula, M. S. Spotz, and D. E. Quinn, "Uniform Waveguide Dispersion Segmented-Core Designs for Dispersion-Shifted Single-Mode Fibers," Conference on Optical Fiber Communications (OFC '84), January 23-25, 1984, New Orleans, *Technical Digest*, pp. 20-21.
31. T. D. Croft, J. E. Ritter, and V. A. Bhagavatula, "Low-Loss Dispersion-Shifted Single-Mode Fiber Manufactured by the OVD Process," Conference on Optical Fiber Communication (OFC '85), February 11-13, 1985, San Diego, *Technical Digest*, pp. 94-95.
32. D. M. Cooper et al., "Multiple-Index Structures for Dispersion-Shifted Single-Mode Fibers," Conference on Optical Fiber Communication (OFC '85), February 11-13, 1985, San Diego, *Technical Digest*, pp. 96-97.
33. D. M. Cooper et al., "Dispersion Shifted Single-Mode Fibres using Multiple Index Structures," *British Telecom Technology Journal*, Vol. 3, April 1985, pp. 52-58.

Biographies (continued)

Material Engineering and Chemistry Department. He joined AT&T in 1979 and currently works on fiber design and preform fabrication, in particular on dispersion-modified and polarization-preserving fibers. He received the B.S. in atmospheric physics from National Central University, Republic of China, and the M.S. and Ph.D. in physics from the University of Illinois at Urbana-Champaign.

(Manuscript received March 26, 1986)